Topological Green function of interacting systems

Minh-Tien Tran,[1] Duong-Bo Nguyen,[2] Hong-Son Nguyen,[3] and Thanh-Mai Thi Tran[1]
[1]*Institute of Physics, Vietnam Academy of Science and Technology, Hanoi 10072, Vietnam*
[2]*Graduate University of Science and Technology, Vietnam Academy of Science and Technology, Hanoi 10072, Vietnam*
[3]*Department of Occupational Safety and Health, Trade Union University, Hanoi 10000, Vietnam*

(Received 3 May 2021; accepted 25 March 2022; published 7 April 2022)

We construct a single-particle Green function, which can identify topological phases of interacting systems. The Green function is defined by an effective Bloch Hamiltonian, which is equal to the inverse of the full Green function of interacting particles at zero frequency. Topological phases of interacting systems can be detected by the coincidence of the poles and the zeros of the diagonal components of the constructed Green function. The crosses of the zeros in the momentum space are also a signal of nontrivial topological phases. As a demonstration, we identify the topological phases in a minimal model of magnetic insulators. The model describes the double exchange process between itinerant electrons and magnetic moments in the presence of the spin-orbital coupling and the ionic potential of the itinerant electrons. The identification of topological phases by the zero's crosses is consistent with the topological invariant. We also found an antiferromagnetic state with topologically breaking of the spin symmetry, where electrons with one spin orientation are in topological insulating state, while electrons with the opposite spin orientation are in topologically trivial one.

DOI: 10.1103/PhysRevB.105.155112

I. INTRODUCTION

Topological phases of interacting systems have attracted a lot of research attention [1,2]. The long-range ordering established by the particle interactions may intriguingly impact on the topology of the ground state, and as a result exotic states may emerge. One of the most fundamental methods for solving the many-body problem of interacting particles is the Green function method [3]. It has widely been used and has many successful applications, ranging from high-energy physics to condensed matters. While the dynamics of interacting systems can closely be determined by the Green function, the presence of particle interactions complicates determining the topological invariant. When the interactions are present, the Hamiltonian of the systems is no longer the single-particle one, and it cannot define the topological invariant in the same way as the noninteracting Hamiltonian does. However, the topological invariant can still be expressed in terms of the single-particle Green function, but the general formulas for the topological invariant are rather complicated [4–7]. Fortunately, they were simplified by using the Green function at zero frequency [8–10]. The inverse of the Green function at zero frequency can play like an effective single-particle Bloch Hamiltonian, that could define the topological invariant of interacting systems [8–10]. This approach has widely been used to identify the topological phases of interacting systems [1,11–17]. Alternatively, the role of the zeros and poles of the single-particle Green function in the relation with the topological phase transition was also noticed [18–21]. The topological invariant corresponds to the zeros of the Green function at the edge, and one can use the zeros to identify the topological phases in interacting systems [18–21].

Recently, a fundamental relation between the eigenvectors and the eigenvalues of Hermitian operator is rediscovered [22]. The eigenvector-eigenvalue relation shows the equivalence between the vanishing of the Bloch wave function and the coincidence of the poles and the zeros of the diagonal components of the Green function in the noninteracting systems [22,23]. On the other hand, the zero points of the Bloch wave function are the source of nontrivial topology of the systems. In particular, in two-dimensional gapped systems, they give nonzero integer contributions to the quantum Hall conductivity [24–26]. Misawa and Yamaji showed a close relation between the coincidence of the poles and the zeros of the diagonal components of the Green function and the zero's crosses in the momentum space [23]. Therefore, the crosses of the zeros of the diagonal components of the Green function can be used as a signal of nontrivial topology [23]. This approach can be used as an alternative and simple method to identify the topological states. The zero's crosses are more simply determined and analyzed than the topological invariant or edge modes. However, the approach is limited to the noninteracting systems.

The aim of the present paper is twofold. First, we extend the approach, proposed by Misawa and Yamaji, to interacting systems. We construct a single-particle Green function, which can determine the topological phases of interacting systems. It is defined by an effective Bloch Hamiltonian, which is equal to the inverse of the original Green function at zero frequency. The coincidence of the poles and the zeros of the diagonal components of the constructed Green function in the momen-

tum space is the source of nontrivial topology of interacting systems. The zero's crosses in the momentum space can be used to identify the topological phases of interacting systems. In interacting systems, the topological invariant or the edge modes are not simply determined and analyzed. However, the momentum dependence of the zeros or the poles of the diagonal components of the constructed Green function is simply determined and analyzed. The topological phase identification by the zeros behavior is an alternative and simple method to investigate the topology of interacting systems. In contrast to the previous studies [18–21], where the zero-energy zeros of the full Green function of interacting particles are used to determine the topological phases, in our proposed approach, the nontrivial topology of interacting systems is determined by the zeros of the generalized Bloch wave function, and it is consistent with the crosses of the zeros of the diagonal components of the constructed Green function in the momentum space. In addition, in contrast to the zeros of the Green function, the zeros the diagonal components of the constructed Green function are still present in the noninteracting case [23]. The second aim of the present paper is to investigate the topological phases of magnetic insulators in the presence of the spin-orbital coupling (SOC). The magnetic topological insulators (MTIs) have attracted a lot of research attention due to the emergence of nontrivial topology and magnetism as well as the high potential of their applications in science and technology [27,28]. The spontaneous magnetization can play like an external magnetic field, and it can give rise to the quantum anomalous Hall effect [27,28]. In the previous studies, we proposed a minimal model for the MTIs [13,14]. It is based on the Kane-Mele and the double exchange models [29,30]. In the proposed model, the SOC causes a topologically nontrivial insulating state, while the spin exchange between itinerant electrons and magnetic moments gives rise to a magnetic ordering [13,14]. The interplay between the SOC and the spin exchange results in the coexistence of nontrivial topology and magnetism. In particular, the quantum spin Hall (QSH) effect is observed in the antiferromagnetic state [13,14]. However, in the previous studies the ionic potential of itinerant electrons was not considered [13,14]. It is originally present in the Kane-Mele model [29]. The ionic potential breaks the sublattice symmetry and drives the topological insulator to topologically trivial one [29]. Both the spin exchange and the ionic potential preserve the topological symmetry between the electron spin orientations, i.e., electrons of both spin orientations simultaneously form either topological or topologically trivial insulators [13,29]. However, we find that the mutual interplay between the ionic potential and the spin exchange can give rise to a topologically breaking of the spin symmetry. Electrons with one spin orientation form a topological insulator, while electrons with the opposite spin orientation form another topologically trivial insulator. As a demonstration of the proposed method, we identify the topological phases by the crosses of the zeros of the diagonal components of the proposed Green function. The phase topology identification is consistent with the topological invariant of the phases.

The paper is organized as follows. In Sec. II we construct a single-particle Green function, which can describe the topological nature of interacting systems. In Sec. III we present a demonstration of using the topological Green function to identify the topological nature of magnetic insulators. Finally, the conclusions are presented in Sec. IV.

II. TOPOLOGICAL GREEN FUNCTION

We consider a general many-body interacting fermion system. We assume that Hamiltonian of the system can be separated into noninteracting and interacting parts, i.e.,

$$H = H_0 + H_1, \tag{1}$$

where H is Hamiltonian of the system, and H_0 (H_1) is its noninteracting (interacting) part. We also assume that the noninteracting Hamiltonian is quadratic, i.e.,

$$H_0 = \sum_{i\alpha,j\beta} c^\dagger_{i\alpha} h_{i\alpha,j\beta} c_{j\beta}, \tag{2}$$

where $c^\dagger_{i\alpha}$ ($c_{i\alpha}$) is the creation (annihilation) operator for fermion at lattice site i with quantum index α. α may include the spin, orbital, sublattice... indices. When the periodic boundary conditions of the lattice are imposed, the noninteracting Hamiltonian can be rewritten in the momentum space

$$H_0 = \sum_{\mathbf{k},\alpha\beta} c^\dagger_{\mathbf{k}\alpha} h_{\alpha\beta}(\mathbf{k}) c_{\mathbf{k}\beta}. \tag{3}$$

$\hat{h}(\mathbf{k})$ is the so-called Bloch Hamiltonian (we use the hat symbol to denote the matrix form). The fermion dynamics can be analyzed through the Green function. We consider the Matsubara Green function

$$G_{i\alpha,j\beta}(i\omega) = -\int d\tau \langle \mathcal{T} c_{i\alpha}(\tau) c^\dagger_{j\beta} \rangle e^{i\omega\tau}, \tag{4}$$

where $i\omega$ is the (imaginary) Matsubara frequency. In the zero-temperature limit the discrete Matsubara frequency becomes continuous. The noninteracting Green function can be represented through the eigenvectors and eigenvalues of the Bloch Hamiltonian

$$g_{i\alpha,j\beta}(i\omega) = \left[\frac{1}{i\omega\hat{1} - \hat{h}}\right]_{i\alpha,j\beta} = \sum_n \frac{\psi_n^{(i\alpha)} \left[\psi_n^{(j\beta)}\right]^*}{i\omega - e_n}, \tag{5}$$

where $\psi_n^{(j\beta)}$ is the $(j\beta)$th component of the eigenvector $\hat{\psi}_n$ of $\hat{h}$ and e_n is its corresponding eigenvalue, i.e.,

$$\hat{h}\hat{\psi}_n = e_n \hat{\psi}_n. \tag{6}$$

In the momentum space, the noninteracting Green function reads

$$g_{\alpha\beta}(\mathbf{k}, i\omega) = \left[\frac{1}{i\omega\hat{1} - \hat{h}(\mathbf{k})}\right]_{\alpha\beta} = \sum_n \frac{\psi_n^{(\alpha)}(\mathbf{k}) \left[\psi_n^{(\beta)}(\mathbf{k})\right]^*}{i\omega - e_n(\mathbf{k})}, \tag{7}$$

where $\hat{\psi}_n(\mathbf{k})$ and $e_n(\mathbf{k})$ are the eigenvector and eigenvalue of $\hat{h}(\mathbf{k})$

$$\hat{h}(\mathbf{k})\hat{\psi}_n(\mathbf{k}) = e_n(\mathbf{k})\hat{\psi}_n(\mathbf{k}). \tag{8}$$

$\hat{\psi}_n(\mathbf{k})$ is just the Bloch wave function, and $e_n(\mathbf{k})$ describes the energy band of noninteracting fermions. The formula in

Eq. (5) or in Eq. (7) is just the single-particle representation of the noninteracting Green function. It describes the single-particle dynamics of the noninteracting systems. Recently, Misawa and Yamaji showed that the diagonal components of the Green function $g_{\alpha\alpha}(\mathbf{k}, i\omega)$ can determine the topological states of the noninteracting systems [23]. In the momentum space, some poles and zeros of the diagonal components of the Green function coincide at the zero points of the Bloch wave function. Because the zero points of the Bloch wave function are the source of nontrivial topology of the systems [23–25], the coincidence of the poles and the zeros of the diagonal components of the Green function in the momentum space can be used to identify the topological phases. When the poles and the zeros coincide, they also guarantee the crosses of the zeros in the momentum space [23]. Therefore, the zero's crosses can also be used to detect the topological states of the noninteracting systems.

In the presence of interactions, we construct a Green function in the single-particle representation

$$\widetilde{G}_{i\alpha,j\beta}(i\omega) = \sum_n \frac{\Psi_n^{(i\alpha)}\left[\Psi_n^{(j\beta)}\right]^*}{i\omega - E_n}, \tag{9}$$

where $\hat{\Psi}_n$ are required to be orthonormal, i.e.,

$$\hat{\Psi}_n^\dagger \hat{\Psi}_m = \sum_{i\alpha} \left[\Psi_n^{(i\alpha)}\right]^* \Psi_m^{(i\alpha)} = \delta_{nm}. \tag{10}$$

In contrast to the noninteracting case, both $\hat{\Psi}_n$ and E_n are yet unknown. They are determined from the condition that the Green function in Eq. (9) satisfies the Dyson equation

$$\widetilde{\hat{G}}(i\omega) = \hat{g}(i\omega) + \hat{g}(i\omega)\hat{\Sigma}(i\omega)\widetilde{\hat{G}}(i\omega), \tag{11}$$

where $\hat{\Sigma}(i\omega)$ is the self energy, which contains all interaction effects. Inserting the single-particle representation (9) into the Dyson equation (11), we obtain

$$\sum_{l\gamma}[h_{i\alpha,l\gamma} + \Sigma_{i\alpha,l\gamma}(i\omega)]\Psi_m^{(l\gamma)} = E_m \Psi_m^{(i\alpha)}. \tag{12}$$

It turns out that $\hat{\Psi}_m$ and E_m are just the eigenvector and eigenvalue of $[\hat{h} + \hat{\Sigma}(i\omega)]$. One can notice that Eq. (12) is valid for any frequency ω, and in general, both $\hat{\Psi}_m$ and E_m depend on ω. However, Eq. (12) does not always have a solution, which satisfies the orthonormality condition in Eq. (10). Therefore, the constructed Green function in Eq. (9) does not always exist. The orthonormality condition in Eq. (10) is mandatory, because without it, Eq. (12) cannot be obtained. However, solutions $\hat{\Psi}_m$ and E_m of Eq. (12), that satisfy the orthonormality condition, may exist at some particular ω. In these cases, the constructed Green function $\widetilde{\hat{G}}(i\omega)$ is equal to the original Green function $\hat{G}(i\omega)$ at the particular ω. If we set $i\omega = E_m$ in the self energy, Eq. (12) becomes the so-called quasiparticle equation [31]:

$$\sum_{l\gamma}[h_{i\alpha,l\gamma} + \Sigma_{i\alpha,l\gamma}(E_m)]\Psi_m^{(l\gamma)} = E_m \Psi_m^{(i\alpha)}. \tag{13}$$

This equation may have several solutions and E_m are the poles of the original Green function $\hat{G}(i\omega)$. The Green function defined by the single-particle representation in Eq. (9) with solutions $\hat{\Psi}_m$ and E_m of Eq. (13) is just the quasiparticle approximation of the original Green function [31]. It describes the quasiparticle dynamics of interacting systems. If we take the limit $\omega \to 0$ in the self energy, Eq. (12) becomes

$$\sum_{l\gamma}[h_{i\alpha,l\gamma} + \Sigma_{i\alpha,l\gamma}(i0)]\Psi_m^{(l\gamma)} = E_m \Psi_m^{(i\alpha)}. \tag{14}$$

One can prove that $\hat{\Sigma}(i0)$ is Hermitian [8–10]. Therefore the eigenvalues E_m are real and the eigenvectors $\hat{\Psi}_m$ can satisfy the orthonormality condition. $\hat{H}^{\text{topo}} \equiv \hat{h} + \hat{\Sigma}(i0) = -\hat{G}^{-1}(i0)$ is called topological Hamiltonian. It can define the topological invariant of interacting systems in the same way as the noninteracting Bloch Hamiltonian does [8–10]. In the momentum space, Eq. (14) reads

$$[\hat{h}(\mathbf{k}) + \hat{\Sigma}(\mathbf{k}, i0)]\hat{\Psi}_m(\mathbf{k}) = E_m(\mathbf{k})\hat{\Psi}_m(\mathbf{k}). \tag{15}$$

$\hat{\Psi}_m(\mathbf{k})$ can be considered as a generalized Bloch wave function of the topological Hamiltonian. The Green function, defined by the single-particle representation in Eq. (9) with eigenvectors $\hat{\Psi}_m(\mathbf{k})$ and eigenvalues $E_m(\mathbf{k})$ of $\hat{H}^{\text{topo}}(\mathbf{k})$ can be rewritten as

$$\widetilde{\hat{G}}^{\text{topo}}(\mathbf{k}, z) = \sum_m \frac{\hat{\Psi}_m(\mathbf{k})\hat{\Psi}_m^\dagger(\mathbf{k})}{z - E_m(\mathbf{k})} = \frac{1}{z\hat{1} - \hat{H}^{\text{topo}}(\mathbf{k})}. \tag{16}$$

$\widetilde{\hat{G}}^{\text{topo}}(\mathbf{k}, z)$ is called "topological Green function" [9,17]. One can use $\widetilde{\hat{G}}^{\text{topo}}(\mathbf{k}, z)$ to calculate the topological invariant of interacting systems [8]. In particular, in two-dimensional insulators, the Hall conductivity calculated by the Kubo formula with $\widetilde{\hat{G}}^{\text{topo}}(\mathbf{k}, z)$ is equal to the one of the original interacting system [8,26].

One can notice that in the noninteracting case, the Green function, the quasiparticle Green function and the topological Green function are identical. In some cases, where the self energy is independent on frequency, for example in the Hartree-Fock approximation, these Green functions are also identical. However, in general, they are different when the particle interactions are present. The topological Green function has the single-particle representation and the topological Hamiltonian is Hermitian, therefore the properties of the topological Green function are similar to the ones of the noninteracting Green function. In particular, the diagonal components of the topological Green function also satisfy

$$\widetilde{G}_{\alpha\alpha}^{\text{topo}}(\mathbf{k}, z) = \sum_n \frac{\left|\Psi_n^{(\alpha)}(\mathbf{k})\right|^2}{z - E_n(\mathbf{k})} = \frac{\prod_l \left[z - \mathcal{E}_l^{(\alpha)}(\mathbf{k})\right]}{\prod_l [z - E_l(\mathbf{k})]}, \tag{17}$$

where $\mathcal{E}_l^{(\alpha)}(\mathbf{k})$ is the lth eigenvalue of the minor $\hat{M}^{(\alpha)}(\mathbf{k})$, which is generated by removing the αth row and column of $\hat{H}^{\text{topo}}(\mathbf{k})$ [22,23]. Equation (17) shows that $\mathcal{E}_l^{(\alpha)}(\mathbf{k})$ is also the zero of the diagonal topological Green function $\widetilde{G}_{\alpha\alpha}^{\text{topo}}(\mathbf{k}, z)$. The eigenvectors and the eigenvalues of $\hat{H}^{\text{topo}}(\mathbf{k})$ also satisfy the following relation [22,23]:

$$\left|\Psi_n^{(\alpha)}(\mathbf{k})\right|^2 = \frac{\prod_l \left[E_n(\mathbf{k}) - \mathcal{E}_l^{(\alpha)}(\mathbf{k})\right]}{\prod_{l\neq n}\left[E_n(\mathbf{k}) - E_l(\mathbf{k})\right]}. \tag{18}$$

This equation shows when $|\Psi_n^{(\alpha)}(\mathbf{k})|^2 = 0$, some poles and zeros of the diagonal topological Green function coincide and vice versa. In gapped systems, the zero points of $\Psi_n^{(\alpha)}(\mathbf{k})$ give

nonzero contributions to the topological invariants determined by $\hat{H}^{\text{topo}}(\mathbf{k})$ [24,25]. Therefore, the topological phases of interacting insulators can also be determined by the coincidence of the poles and the zeros of the diagonal components of the topological Green function. When the poles and the zeros coincide, they also guarantee the crosses of the zeros in the momentum space [23]. This allows us to use the zero's crosses in the momentum space to identify the topological phases of interacting insulators. The topological Green function for interacting systems was previously noticed [9,17]. However, in contrast to the previous studies, only its diagonal components are relevant to the topological phase identification through the coincidence their poles and zeros. When the self energy is determined, the momentum dependence of the zeros can be obtained and analyzed more simply than direct calculations of the topological invariants or edge modes.

The topological Green function can also determine the topological phases of interacting gapless systems [17]. In the gapless systems such as the Weyl or Dirac semimetals, the energy bands touch or cross at the gapless points. The topological gapless points of interacting semimetals are also determined by the touch points of the eigenvalues of the topological Hamiltonian [17]. From the Cauchy interlacing inequalities [23]

$$E_l(\mathbf{k}) \leqslant \mathcal{E}_l^{(\alpha)}(\mathbf{k}) \leqslant E_{l+1}(\mathbf{k}), \tag{19}$$

one can notice that the zeros of the diagonal topological Green function also touch at the gapless points. Therefore, we can also detect the gapless points by the zeros. However, in addition to the topological gapless points, the zeros may accidentally touch or cross at high symmetry points of the Brillouin zone. This additionally requires a careful selection of the topological gapless points from the zero's behavior. However, if the zeros do not touch or cross, the interacting systems are definitely not gapless.

The quasiparticle Green function also has the single-particle representation, but its effective Hamiltonian may be not Hermitian. Therefore the eigenvector-eigenvalue relation may not be valid, and the poles and the zeros of the quasiparticle Green function may not coincide at the zero points of the generalized Bloch wave function. However, it seems that the quasiparticle Green function can still describe the topology of interacting particles at exceptional points or in open systems [32–34].

III. TOPOLOGICAL PHASES IN MAGNETIC INSULATORS

We consider a minimal model for MTIs [13,14]. It consists of a tight binding model of electrons in the presence of the intrinsic SOC and magnetic impurities. The intrinsic SOC may give rise to a topological insulating state. A spontaneous magnetization may occur as a consequence of the spin exchange between electrons and magnetic impurities. The model Hamiltonian reads

$$\begin{aligned} H = &-t \sum_{\langle i,j\rangle,\sigma} c_{i\sigma}^{\dagger} c_{j\sigma} - i\lambda \sum_{\langle\langle i,j\rangle\rangle,s,s'} \nu_{ij} c_{is}^{\dagger} \sigma_{ss'}^{z} c_{js'} \\ &- \frac{\Delta}{2} \sum_{i\sigma} \epsilon_i c_{i\sigma}^{\dagger} c_{i\sigma} - J \sum_{i,ss'} \mathbf{S}_i c_{is}^{\dagger} \boldsymbol{\sigma}_{ss'} c_{is'}, \end{aligned} \tag{20}$$

where $c_{i\sigma}^{\dagger}$ ($c_{i\sigma}$) is the creation (annihilation) operator for electron with spin σ at site i of a honeycomb lattice. $\langle i, j\rangle$ and $\langle\langle i, j\rangle\rangle$ denote the nearest-neighbor and next-nearest-neighbor lattice sites, respectively. t is the hopping parameter for the nearest-neighbor sites, and λ is the strength of the intrinsic SOC. The sign $\nu_{ij} = \pm 1$ when the hopping direction is anticlockwise (clockwise) [29]. The honeycomb lattice is divided into two penetrating sublattices a and b. $\epsilon_i = \pm 1$ when the lattice site i belongs to the sublattice a (b). Δ is a staggered ionic potential, which breaks the sublattice symmetry of the honeycomb lattice. $\mathbf{S}_i$ is spin of magnetic impurity at lattice site i. $\boldsymbol{\sigma} = (\sigma^x, \sigma^y, \sigma^z)$ are the Pauli matrices. J is the spin exchange between conduction electrons and magnetic impurities. When the spin exchange $J = 0$, the model in Eq. (20) is reduced to the Kane-Mele model [29]. The SOC opens a gap and induces the QSH state, where the spin Hall conductivity is quantized [29]. The ionic potential drives the phase transition between the QSH state and topologically trivial band insulator [29]. When $\lambda = 0$ and $\Delta = 0$, the Hamiltonian in Eq. (20) describes the double exchange of electrons [30]. The spin exchange drives the system from paramagnetic to magnetic states [30]. The double-exchange model was widely used to study the magnetic phases in a number of materials, including the maganites, kagome magnets and related compounds [35–39]. We treat the spin of magnetic impurities $\mathbf{S}_i$ as the classical spin, and this rules out the Kondo effect. In addition, the ferromagnetic spin exchange ($J > 0$) does not favour the Kondo singlet formation [40]. The antiferromagnetic spin exchange ($J < 0$) may give rise to the competition between the Kondo singlet formation and magnetic interactions [41]. However, the Kondo singlet formation are hardly present in magnetic topological insulators, and we do not consider the Kondo effect and related phenomena here. When the ionic potential is absent ($\Delta = 0$), the spin exchange and the SOC mutually interplay, and as a consequence the model in Eq. (20) exhibits a magnetic topological phase transition at half filling [13]. With a fixed SOC, the spin exchange drives the system from the paramagnetic topological (QSH) state to an antiferromagnetic topological (QSH) state, and then to a topologically trivial antiferromagnetic state [13]. We will examine the mutual effect of the ionic potential and the spin exchange on the magnetic topological phase transition at half filling. In the following we use $t = 1$ as the unit of energy.

We use the dynamical mean field theory (DMFT) to calculate the Green function and its self energy [42,43]. The DMFT is widely and successfully applied to correlated electron systems, including the double-exchange model [35–37]. Within the DMFT, the self energy only depends on frequency. Therefore, the Dyson equation of the Green function reads

$$\hat{G}(\mathbf{k}, z) = [z - \hat{H}_0(\mathbf{k}) - \hat{\Sigma}(z)]^{-1}, \tag{21}$$

where $\hat{G}(\mathbf{k}, z)$ and $\hat{\Sigma}(z)$ is the Green function and the self energy of electrons. Here, we represent the creation operator for electrons in the row vector with the spin and the sublattice indices $(c_{\mathbf{k}a\uparrow}^{\dagger}, c_{\mathbf{k}b\uparrow}^{\dagger}, c_{\mathbf{k}a\downarrow}^{\dagger}, c_{\mathbf{k}b\downarrow}^{\dagger})$ [13]. The Green function $\hat{G}(\mathbf{k}, z)$ and the self energy $\hat{\Sigma}(z)$ are 4×4 matrices. $\hat{H}_0(\mathbf{k})$ is the noninteracting Bloch Hamiltonian, which has the block

form in the spin index

$$\hat{H}_0(\mathbf{k}) = \begin{pmatrix} \hat{h}_\uparrow(\mathbf{k}) & 0 \\ 0 & \hat{h}_\downarrow(\mathbf{k}) \end{pmatrix}, \tag{22}$$

where

$$\hat{h}_\sigma(\mathbf{k}) = \begin{pmatrix} -\sigma\lambda\xi_\mathbf{k} - \Delta/2 & -t\gamma_\mathbf{k} \\ -t\gamma_\mathbf{k}^* & \sigma\lambda\xi_\mathbf{k} + \Delta/2 \end{pmatrix}.$$

Here we have used the following notations: $\gamma_\mathbf{k} = \sum_\delta e^{i\mathbf{k}\cdot\mathbf{r}_\delta}$, $\xi_\mathbf{k} = i\sum_\eta \nu_\eta e^{i\mathbf{k}\cdot\mathbf{r}_\eta}$, where δ and η denote nearest-neighbor and next-nearest-neighbor sites of a given site in the honeycomb lattice. Within the DMFT the self energy is diagonal $\hat{\Sigma}(z) = \mathrm{diag}[\Sigma_{a\uparrow}(z), \Sigma_{b\uparrow}(z), \Sigma_{a\downarrow}(z), \Sigma_{b\downarrow}(z)]$, because the DMFT neglects intersite correlations. Therefore, the Green function also has the block form in the spin index. This allows us to consider the electron dynamics and topology in each spin sector. In the strong coupling regime ($J \gg t, \lambda$) and in the nonfrustrated lattices, the strong spin exchange between electrons and magnetic impurities favors the magnetic ordering in the z-axis direction [13]. However, the lattice frustration may favor noncollinear magnetic states [44,45]. The self energy $\Sigma_{\alpha\sigma}(z)$ is calculated from a single site of the α-sublattice embedded in a self-consistent dynamical mean field [13]. For classical spin of magnetic impurities, the effective single site can exactly be solved and the self energy can self consistently be determined [13]. Without loss of generality, we set the magnitude of the impurity spin $S = 1$. Once the self energy and the Green function are obtained, we can compute the magnetization and determine the magnetic nature of the ground state. The magnetization of the α sublattice is determined by

$$m_\alpha = \frac{1}{2N}\sum_{\mathbf{k},\sigma} \sigma \langle c^\dagger_{\mathbf{k}\alpha\sigma} c_{\mathbf{k}\alpha\sigma}\rangle, \tag{23}$$

which can directly be calculated from the Green function in Eq. (21). When $m_a = m_b \neq 0$, the ground state is ferromagnetic, and when $m_a = -m_b \neq 0$ it is antiferromagnetic. The Chern number can also be computed by the generalized Thouless-Kohmoto-Nightingale-den Nijs formula

$$C_\sigma = \frac{1}{2\pi}\int d^2k \mathcal{F}^{xy}_\sigma(\mathbf{k}), \tag{24}$$

where $\mathcal{F}^{ab}_\sigma(\mathbf{k}) = \partial_{k_a}\mathcal{A}^b_\sigma(\mathbf{k}) - \partial_{k_b}\mathcal{A}^a_\sigma(\mathbf{k})$, $\mathcal{A}^a_\sigma(\mathbf{k}) = i\sum_{m:E_{m\sigma}(\mathbf{k})<0} [\hat{\Psi}^\dagger_{m\sigma}(\mathbf{k})\partial_{k_a}\hat{\Psi}_{m\sigma}(\mathbf{k})]$ [8,26]. A nonzero integer value of C_σ implies a topologically nontrivial insulating state of electrons with spin σ, while $C_\sigma = 0$ indicates a topologically trivial one. The Chern number can numerically be calculated by using the efficient computing method [46].

We consider the regime, where the ground state is the Z_2 topological insulator at $J = 0$ [29]. In Fig. 1 we plot the dependence of the sublattice magnetizations and the Chern number on the spin exchange J for each spin orientation. Figure 1 shows a critical spin exchange J_m

(for $\lambda = 0.5$ and $\Delta = 1$, $J_m \approx 0.6$), which separates the antiferromagnetic ground state ($m_a = -m_b \neq 0$) from the paramagnetic one ($m_a = m_b = 0$). The magnetic phase transition is a common feature of the double exchange model [30,35,37–39]. The SOC and the ionic potential do not qualitatively change the phase transition. However, the Chern numbers significantly change when the ionic potential is present. Figure 1 shows three different topological regions,

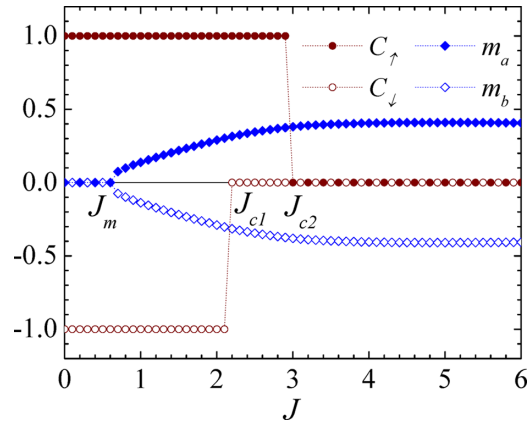

FIG. 1. The Chern number C_σ for spin orientation σ and the sublattice magnetization m_α via the spin exchange J at fixed SOC $\lambda = 0.5$ and ionic potential $\Delta = 1$.

which are separated by J_{c1} and J_{c2} (for $\lambda = 0.5$ and $\Delta = 1$, $J_{c1} \approx 2.2$, $J_{c2} \approx 3.0$). When $J < J_{c1}$, the Chern number $C_\uparrow = -C_\downarrow = 1$. In this region the charge Hall conductivity vanishes, while the spin one is quantized. It is the SQH effect. When $J_{c1} < J < J_{c2}$, electrons with different spin orientations have different topological invariants. Electrons with spin up form a Chern topological insulator with $C_\uparrow = 1$, while electrons with spin down are in topologically trivial insulating state ($C_\downarrow = 0$). This shows a topologically breaking of the spin symmetry. Only when $\Delta \to 0$, $J_{c1} = J_{c2}$, the topological symmetry of two spin orientations is restored. It indicates an essential role of the ionic potential in the topologically breaking. However, the ionic potential alone cannot break the topological symmetry of two spin orientations, because in the absence of the spin exchange, two spin orientations are topologically symmetric, i.e., electrons with both spin orientations simultaneously form either topological or topologically trivial insulators [29]. When $J > J_{c2}$, electrons with both spin orientations are in topologically trivial insulator, because $C_\uparrow = C_\downarrow = 0$.

The topological states can also be detected by the crosses of the zeros of the diagonal components of the topological Green function. In contrast to the Chern number, the zeros are simply determined and analyzed. We obtain the analytical expression of the zeros

$$\mathcal{E}^{(\alpha)}_\sigma(\mathbf{k}) = -\epsilon_{\bar{\alpha}}\sigma\lambda\xi_\mathbf{k} - \epsilon_{\bar{\alpha}}\Delta/2 + \Sigma_{\bar{\alpha}\sigma}(i0), \tag{25}$$

where the sublattice index $\bar{\alpha} = b, a$ when $\alpha = a, b$, respectively. In Fig. 2 we plot the zeros of the diagonal topological Green function and the spectral functions $\rho_{a\sigma}(\mathbf{k}, \omega) = -\mathrm{Im}G_{\alpha\sigma}(\mathbf{k}, \omega + i0^+)/\pi$ in the three typical topological phase regions. The peaks of the spectral functions resemble the quasiparticles and describe the energy bands. Figure 2 shows that the spectral functions clearly display upper and lower bands separated by a gap for all values of J. Both the SOC and the spin exchange open the gap [13]. However, the spin exchange first reduces the band gap opened by the SOC, and then increases the band gap after closing it [13]. The gapless points are the evidence of the topological phase transition. In the region of weak spin exchange $J < J_{c1}$, in both spin sectors the zeros cross each other as shown in Fig. 2. The zero's crosses are the evidence of a topological state, because

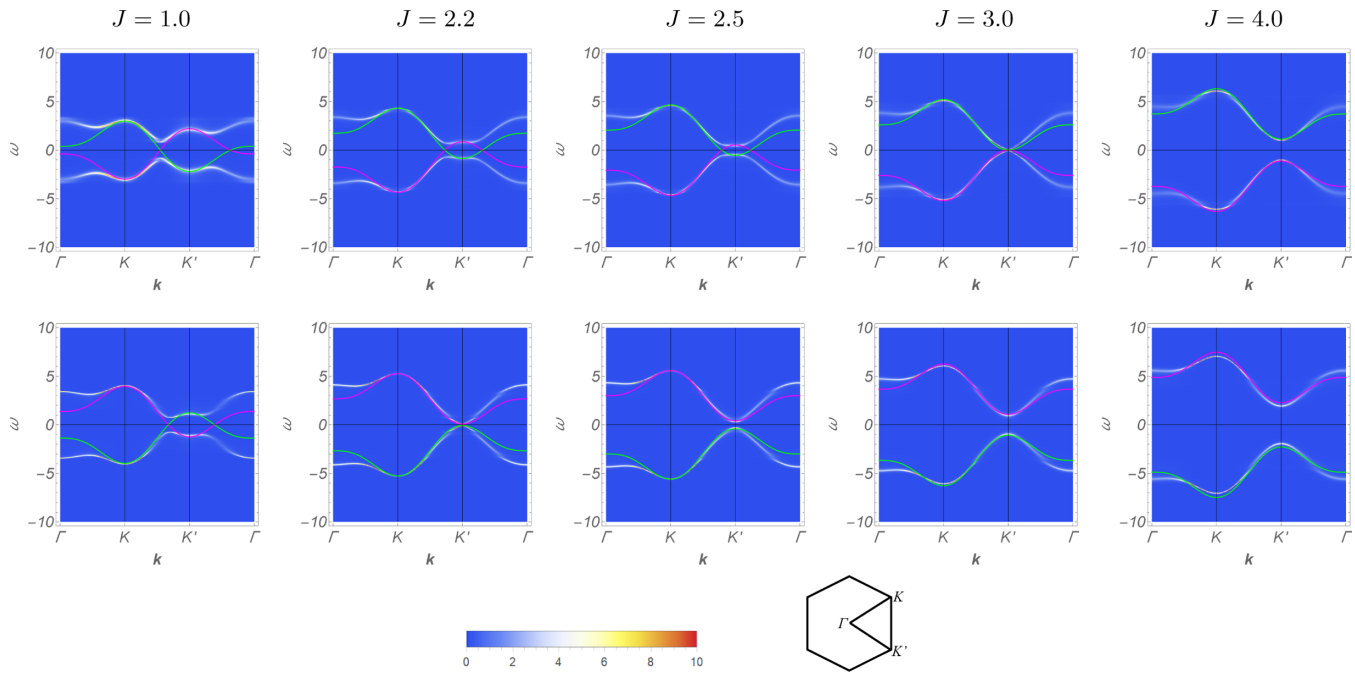

FIG. 2. The spectral function of electrons (the color density plot) and the zeros of the diagonal topological Green function (the green and magenta solid lines) along the high symmetry lines of the Brillouin zone for various values of the spin exchange J and fixed SOC $\lambda = 0.5$ and $\Delta = 1$. The upper (lower) row presents the plots for the spin up (down) orientation. Due to the overlap between the spectral functions of two sublattices, the color density plots show the maximum values between the sublattice spectral functions.

they are a consequence of the coincidence of the poles and zeros, or equivalently, of the existence of the zero points of the generalized Bloch wave function of the topological Hamiltonian. Therefore, electrons with both spin orientations are in the topological insulating state. However, the zero's crosses alone cannot reveal the value of the Chern numbers. Because this region adiabatically connects with the Z_2 topological insulator at $J = 0$, the ground state could be the QSH one. In the intermediate region $J_{c1} < J < J_{c2}$, in the spin-up sector, the zeros cross each other, while in the spin-down sector they do not cross. This implies that electrons with spin up form a Chern topological insulator, and electrons with spin down are in a topologically trivial insulating state. The cross behavior of the zeros is consistent with the Chern numbers. When the spin exchange is large, $J > J_{c2}$, in both spin sectors the zeros do not cross each other as shown in Fig. 2. This shows that electrons with both spin orientations form topologically trivial insulator. In contrast to the Chern number, the momentum dependence of the zeros is simpler obtained and analyzed. Equation (25) clearly shows that the spin exchange impacts on the momentum dependence of the zeros through the self energy at zero frequency. Within the DMFT, the self energy only shifts the zero's momentum dependence. However, in magnetic states, the shifting of the self energy is spin dependent. In the antiferromagnetic state $\Sigma_{a\uparrow}(i0) - \Sigma_{a\downarrow}(i0) = -[\Sigma_{b\uparrow}(i0) - \Sigma_{b\downarrow}(i0)]$, and the ionic potential plays like a staggered chemical potential, which leads to $\Sigma_{a\uparrow}(i0) + \Sigma_{a\downarrow}(i0) = -[\Sigma_{b\uparrow}(i0) + \Sigma_{b\downarrow}(i0)]$. Therefore, the self energy can be represented as

$$\Sigma_{\alpha\sigma}(i0) = \epsilon_\alpha M + \epsilon_\alpha \sigma \delta M, \tag{26}$$

where $M = [\Sigma_{a\uparrow}(i0) + \Sigma_{a\downarrow}(i0)]/2$, and $\delta M = [\Sigma_{a\uparrow}(i0) - \Sigma_{a\downarrow}(i0)]/2$. Equation (26) shows that the self energy $\Sigma_{\alpha\sigma}(i0)$ plays like a combination of staggered nonmagnetic and magnetic fields. Therefore, in different spin sectors the spin exchange shifts the zeros apart differently. As a consequence, in the intermediate region, the zeros in the spin-down sector do not cross each other, while the zeros in the spin-up sector still cross. This leads to a topologically breaking of the spin orientations. When the spin exchange is absent ($J = 0$), the self energy vanishes, and the ionic potential only describes the phase transition from topological insulator to topologically trivial insulator [29]. When the ionic potential vanishes ($\Delta = 0$), $M = 0$, the topological symmetry of the spin orientations is restored [13]. These limiting cases show that neither the spin exchange nor the ionic potential alone can break the topological symmetry of two spin orientations. The topologically breaking of the spin symmetry is a mutual effect of the spin exchange and the ionic potential. It is a challenge to observe and explore such topologically breaking of the spin symmetry by experiments. Indeed, the Haldane model was experimentally realized by ultracold atoms [47]. One may expect the Kane-Mele model or the spin version of the Haldane model may be realized too. When a staggered field like the self energy in Eq. (26) is imposed over the quantum simulated lattice, the topologically breaking of the spin symmetry would be observed. When the spin exchange is large $J > J_{c2}$, the self energy $\Sigma_{\alpha\sigma}(i0)$ is large enough and it shifts the zeros in both spin sectors away from each other. Therefore, in this region electrons with both spin orientations are in topologically trivial insulator.

At the topological phase transition point J_{c1} (J_{c2}), the spectral functions of the sublattice a and b touch each other,

as shown in Fig. 2. This shows a gapless state in the spin down (up) sector. The occurrence of the gapless state is a consequence of the change of the topological invariant at the phase transition point, and it is an evidence of the bulk-edge correspondence. Figure 2 also shows a touch of the zeros at the topological phase transition. Although the Cauchy interlacing inequalities in Eq. (19) were proved only for the topological Green function, the zero's touch at the gapless points suggests that the Cauchy interlacing inequalities may also be valid at the gapless points for the poles of the full interacting Green function and the zeros of the diagonal topological Green function. However, it requires a further study. Nevertheless, the numerical results show that at the gapless points, the energy bands of interacting fermions, the poles and the zeros of the diagonal topological Green function touch each other. We can use either the energy bands, the poles or the zeros to determine the gapless points, such as the Weyl nodes of the Weyl semimetals [17]. However, except for the gapless points, the zeros of the diagonal topological Green function do not always lie within the band gap, especially when the spin exchange is strong.

IV. CONCLUSION

We have constructed the topological Green function, which can determine the topological phases of interacting fermions. Based on the eigenvector-eigenvalue relation of Hermitian operator, it was shown that the nontrivial topology of the ground state can be detected by the crosses of the zeros of the diagonal components of the topological Green function in the momentum space. The momentum dependence of the zeros is simply determined and analyzed. As an application, we have identified the topological phases in a minimal model of magnetic insulators. It is found that the interplay between the spin exchange and the ionic potential can cause a topologically breaking of the spin symmetry. In the antiferromagnetic state with topologically breaking of the spin symmetry, electrons with one spin orientation form a topological insulator, while electrons with the opposite spin orientation form another topologically trivial one. The topological phase identification by the zero's crosses is consistent with the topological invariant of interacting electrons. However, the zero's crosses can only identify the topological phases and it seems that it cannot reveal the nonzero value of the topological invariant. The topological Green function can also describe the topology of gapless systems. The gapless points can be determined by the zero's touch in the momentum space. In the noninteracting systems, the degeneracy of the zeros corresponds to the degeneracy of the edge states [23]. However, in interacting systems it is not clear that the zero-edge correspondence is still valid, because the topological Green function differs from the full Green function of interacting particles. We leave the problem for further study.

ACKNOWLEDGMENT

This research is funded by Vietnam National Foundation for Science and Technology Development (NAFOSTED) under Grant No. 103.01-2019.309.

[1] M. Hohenadler and F. F. Assaad, J. Phys.: Condens. Matter **25**, 143201 (2013).
[2] S. Rachel, Rep. Prog. Phys. **81**, 116501 (2018).
[3] A. A. Abrikosov, L. P. Gorkov, and I. E. Dzyaloshinski, *Method of Quantum Field Theory in Statistical Physics* (Dover, New York, 1975).
[4] G. E. Volovik, Zh. Eksp. Teor. Fiz. **94**, 123 (1988) [Sov. Phys. JETP **67**, 1804 (1988)].
[5] Z. Wang, X.-L. Qi, and S.-C. Zhang, Phys. Rev. Lett. **105**, 256803 (2010).
[6] L. Wang, X. Dai, and X. C. Xie, Phys. Rev. B **84**, 205116 (2011).
[7] L. Wang, H. Jiang, X. Dai, and X. C. Xie, Phys. Rev. B **85**, 235135 (2012).
[8] Z. Wang and S.-C. Zhang, Phys. Rev. X **2**, 031008 (2012).
[9] Z. Wang and S.-C. Zhang, Phys. Rev. B **86**, 165116 (2012).
[10] Z. Wang and B. Yan, J. Phys.: Condens. Matter **25**, 155601 (2013).
[11] M.-T. Tran, T. Takimoto, and K.-S. Kim, Phys. Rev. B **85**, 125128 (2012).
[12] H.-S. Nguyen and M.-T. Tran, Phys. Rev. B **88**, 165132 (2013).
[13] M.-T. Tran, H.-S. Nguyen, and D.-A. Le, Phys. Rev. B **93**, 155160 (2016).
[14] T.-M. T. Tran, D.-A. Le, T.-M. Pham, K.-T. T. Nguyen, and M.-T. Tran, Phys. Rev. B **102**, 205124 (2020).
[15] R. Peters and T. Yoshida, and N. Kawakami, Phys. Rev. B **98**, 075104 (2018).
[16] T. Mertz, K. Zantout, and R. Valenti, Phys. Rev. B **100**, 125111 (2019).
[17] W. Witczak-Krempa, M. Knap, and D. Abanin, Phys. Rev. Lett. **113**, 136402 (2014).
[18] V. Gurarie, Phys. Rev. B **83**, 085426 (2011).
[19] S. R. Manmana, A. M. Essin, R. M. Noack, and V. Gurarie, Phys. Rev. B **86**, 205119 (2012).
[20] B. Sbierski and C. Karrasch, Phys. Rev. B **98**, 165101 (2018).
[21] R.-J. Slager, L. Rademaker, J. Zaanen, and L. Balents, Phys. Rev. B **92**, 085126 (2015).
[22] P. B. Denton, S. J. Parke, T. Tao, and X. Zhang, Bull. Am. Math. Soc. **59**, 31 (2022).
[23] T. Misawa and Y. Yamaji, arXiv:2102.04665.
[24] Y. Hatsugai, J. Phys.: Condens. Matter **9**, 2507 (1997).
[25] Y. Morita and Y. Hatsugai, Phys. Rev. B **62**, 99 (2000).
[26] D. J. Thouless, M. Kohmoto, M. P. Nightingale, and M. den Nijs, Phys. Rev. Lett. **49**, 405 (1982).
[27] H. Weng, R. Yu, X. Hu, X. Dai, and Z. Fang, Adv. Phys. **64**, 227 (2015).
[28] Y. Tokura, K. Yasuda, and A. Tsukazaki, Nat. Rev. Phys. **1**, 126 (2019).
[29] C. L. Kane and E. J. Mele, Phys. Rev. Lett. **95**, 146802 (2005).
[30] C. Zener, Phys. Rev. **82**, 403 (1951).

[31] L. Hedin and S. Lundqvist, in *Solid State Physics*, edited by F. Seitz, D. Turnbull, and H. Ehrenreich (Academic Press, New York, 1969), Vol. 23, p.1.
[32] H. Shen, B. Zhen, and L. Fu, Phys. Rev. Lett. **120**, 146402 (2018).
[33] T. Yoshida, R. Peters, and N. Kawakami, Phys. Rev. B **98**, 035141 (2018).
[34] J.-H. Zheng and W. Hofstetter, Phys. Rev. B **97**, 195434 (2018).
[35] E. Dagotto, *Nanoscale Phase Separation and Colossal Magnetoresistance*, Springer series in Solid-State Sciences Vol. 136, (Springer, New York, 2003).
[36] Yu. A. Izyumov and Yu. N. Skryabin, Phys. Usp. **44**, 109 (2001).
[37] N. Furukawa, J. Phys. Soc. Jpn. **63**, 3214 (1994); **64**, 2754 (1995); **65**, 1174 (1996).
[38] H. D. Rosales, F. A. Gómez Albarracín, and P. Pujol, Phys. Rev. B **99**, 035163 (2019).
[39] T.-M. T. Tran, D.-B. Nguyen, H.-S. Nguyen, and M.-T. Tran, Mater. Res. Express **8**, 126101 (2021).
[40] S. Capponi and F. F. Assaad, Phys. Rev. B **63**, 155114 (2001).
[41] H. Tsunetsugu, M. Sigrist, and K. Ueda, Rev. Mod. Phys. **69**, 809 (1997).
[42] W. Metzner and D. Vollhardt, Phys. Rev. Lett. **62**, 324 (1989).
[43] A. Georges, G. Kotliar, W. Krauth, and M. J. Rozenberg, Rev. Mod. Phys. **68**, 13 (1996).
[44] K. Ohgushi, S. Murakami, and N. Nagaosa, Phys. Rev. B **62**, R6065 (2000).
[45] A. Rahmani, R. A. Muniz, and I. Martin, Phys. Rev. X **3**, 031008 (2013).
[46] T. Fukui, Y. Hatsugai, and H. Suzuki, J. Phys. Soc. Jpn. **74**, 1674 (2005).
[47] G. Jotzu, M. Messer, R. Desbuquois, M. Lebrat, T. Uehlinger, D. Greif, and T. Esslinger, Nature (London) **515**, 237 (2014).